HHS Public Access

Author manuscript

Trans Soc Min Metall Explor Inc. Author manuscript; available in PMC 2017 June 15.

Published in final edited form as:

Trans Soc Min Metall Explor Inc. 2016 ; 340(1): 30–37.

Measurement of RF propagation around corners in underground mines and tunnels

R. Jacksha and **C. Zhou**

Electronics technician and senior electrical engineer, respectively, Office of Mine Safety and Health Research, National Institute for Occupational Safety and Health, Spokane, WA, and Pittsburgh, PA, USA

Abstract

This paper reports measurement results for radio frequency (RF) propagation around 90° corners in tunnels and underground mines, for vertically, horizontally and longitudinally polarized signals. Measurements of signal power attenuation from a main entry into a crosscut were performed at four frequencies — 455, 915, 2450 and 5800 MHz — that are common to underground radio communication systems. From the measurement data, signal power loss was determined as a function of signal coupling from the main entry into the crosscut. The resultant power loss data show there are many factors that contribute to power attenuation from a main entry into a crosscut, including frequency, antenna polarization and cross-sectional entry dimensions.

Keywords

Radio propagation; Wireless communication; Waveguide; Corner diffraction

Introduction

In response to a series of underground coal mining disasters, the U.S. Congress passed the Mine Improvement and New Emergency Response Act (MINER Act) in 2006. One of the requirements of the MINER Act is for all underground coal mine operators to provide for post-accident communication between underground and surface personnel through a wireless two-way medium and to provide for an electronic tracking system permitting surface personnel to determine the location of any persons trapped underground. Many coal mines have installed communications and tracking systems using radio frequencies in the ultra-high and super-high frequency (UHF/SHF) bands. Frequencies of particular interest are 455, 915, 2450 and 5800 MHz, which represent frequencies used by the Mine Safety and Health Administration's (MSHA) permissibly approved wireless communications and tracking systems.

Corresponding author: rjacksha@cdc.gov.

Disclaimer

The findings and conclusions in this paper are those of the authors and do not necessarily represent the views of NIOSH. The mention of any company name or product does not constitute endorsement by NIOSH.

UHF propagation in mines and tunnels differs significantly from above ground, but the underground behavior is not fully understood and has proven difficult to model. To improve the understanding of and the ability to accurately model UHF propagation, the U.S. National Institute for Occupational Safety and Health's (NIOSH) Office of Mine Safety and Health Research (OMSHR) performed measurements of radio signal propagation in mines. The resultant measurement data are used to enhance both pre- and post-accident performance of communications and tracking systems. OMSHR's propagation measurements have primarily involved "line-of-sight" propagation, where the transmitter and receiver are in a straight line with no obstructions. To better understand how radio signals couple from an entry into a crosscut, OMSHR researchers performed crosscut coupling measurements, also referred to as "around-the-corner" measurements. Along with the line-of-sight propagation measurements, understanding this around-the-corner crosscut coupling mechanism is important for designing and deploying wireless systems in underground mines, which generally consist of entries and crosscuts that can be viewed as perpendicularly intersected tunnels. This paper reports the results of the OMSHR around-the-corner measurements.

Measurement system and methods

Measurement system

The design for the radio frequency (RF) propagation measurement apparatus was driven by the unique environment of the underground coal mine. Ruggedness, portability and simplicity were the goals, targeting a system able to survive the harsh environment of an operating underground mine, yet still able to be easily broken down for transport and quickly set up for use. Materials such as polyvinyl chloride (PVC), carbon fiber, plastic and plywood were used wherever possible in an effort to keep the apparatus RF transparent, thus reducing its influence on the measured RF signal. Finally, all the instruments were required to be battery powered due to the limited availability of mains power in the test areas.

The block diagram of the test apparatus is shown in Fig 1. It is composed of two assemblies: a stationary transmitter and a mobile receiver. The transmitter (Tx) consists of an RF signal source connected to one of four omni-directional J-pole antennas or an RF power meter. The receiver (Rx) includes a data logging spectrum analyzer connected through an RF A/B switch to either a 50 Ω termination or an antenna matching that of the transmitter.

Figure 2 shows the test apparatus. On the left is the transmitter with an antenna shown mounted in vertical polarization on a carbon fiber antenna stand and connected to the RF source with an LMR-400UF coaxial cable. On the right is the cart used for receiver mobility. It was constructed of plywood with plastic wheels, polyurethane tires and a PVC handle, which placed the operator about 2 m (6.6 ft) in front of the Rx antenna during measurements. Like the transmitter, the receiver cart used a carbon fiber antenna stand and was connected to the spectrum analyzer with an LMR-400UF coaxial cable.

Measurement method

RF signal propagation was measured as follows: The RF signal source was configured to produce a continuous wave signal with a fixed output power. An RF power meter was used

to verify power at the Tx antenna end of the coaxial cable at the beginning of each series of measurements for a given frequency. The spectrum analyzer was configured to measure channel power with its input connected to the 50 Ω termination through a microwave A/B switch. To begin a measurement, data logging was started on the spectrum analyzer, its input was switched to the Rx antenna, and the mobile receiver cart was pulled away from the transmitter. At 10-m intervals of distance, the mobile receiver cart was halted and the spectrum analyzer's input was momentarily switched to the 50 Ω termination. This inserted a received power null in the measured data that served as a distance marker. The spectrum analyzer's input was then switched back to the Rx antenna, and travel away from the transmitter was resumed. Post-processing of the logged data was performed to correlate the power nulls in the data to the 10-m intervals.

Measurement configuration

Measurements were performed at the four frequencies of interest — 455, 915, 2450 and 5800 MHz — using an antenna height of 1.2 m (4 ft) for both the Tx and Rx antennas. Given that research has shown there are near- and far-zone regions of propagation in underground mines and tunnels, propagation behavior into a crosscut could vary as function of the Tx antenna's distance from the crosscut (Dudley et al., 2007; Hrovat and Javornik, 2014). Therefore, to ensure measurements were taken with the crosscut in both the near and far zones of propagation, the Tx antenna was placed both near to and far from the crosscut. For entries less than 3 m (10 ft) in width, measurements were made with the Tx antenna located 70 m (230 ft) and 10 m (33 ft) from the centerline of the crosscut. For entries greater than 3 m (10 ft) in width, measurements were made with the Tx antenna located 90 m (295 ft) and 20 m (66 ft) from the crosscut. Figure 3 shows an example of the near- and far-zone regions of line-of-sight propagation in a concrete tunnel measuring 1.8 m (6 ft) wide by 2.4 m (8 ft) high.

Three antenna polarization combinations were used: vertical, horizontal and longitudinal. The concept of longitudinally aligned antennas is as follows: As the receiver cart turns the corner, a horizontally aligned Rx antenna becomes orthogonally aligned to its previous orientation (Fig 4a). For the measurements defined as longitudinal, as the receiver cart turns the corner, the horizontally aligned Rx antenna is rotated 90° on the cart to once again be oriented the same as before the corner was turned (Fig. 4b).

It is important to note that rather than allowing the receiver cart to simply turn the corner on a curved path, when the intersection of the corner was reached, data logging on the spectrum analyzer was paused and the cart was rotated 90°. Once the cart was reoriented, data logging was resumed and travel in the new direction begun.

Testing sites

Around-the-corner propagation measurements were performed at three locations: a small concrete tunnel, a shotcrete-lined small-dimension coal mine, and a high-seam western coal mine.

The concrete tunnel was located within the Grand Coulee Dam in Washington state. The main tunnel (Fig 5) was 1.8 m (6 ft) wide and 2.4 m (8 ft) high, and it had an arched ceiling beginning 1.5 m (5 ft) up the side of the wall. Intersecting the main tunnel was a side tunnel measuring 1.5 m (5 ft) wide by 2.1 m (7 ft) high with an arched ceiling beginning 1.4 m (5 ft) up the wall. The concrete walls were very smooth with a single conduit pipe running along the ceiling.

The shotcrete-lined small-dimension coal mine was NIOSH's Safety Research Coal Mine (SRCM) located south of Pittsburgh, PA. The main entry (Fig. 6) and crosscut were both approximately 2.7 m (9 ft) wide and 1.6 m (5 ft) to 2.0 m (7 ft) high. The ceilings and walls were very rough and covered with shotcrete. Numerous metallic conductors were present: steel support beams under the shotcrete on the ceilings, various electric and communications cables on both walls, and rails on the floor.

The width of the western high-seam coal mine's main entry varied from 5.6 m (18 ft) to 5.9 m (19 ft) and the height ranged from 2.7 m (9 ft) to 3.4 m (11 ft). The crosscut's width varied from 5.2 m (17 ft) to 5.3 m (17 ft) with the height varying from 2.4 m (8 ft) to 2.7 m (9 ft). The walls and floor were heavily rock dusted, and the ceiling was covered with extensive ground control measures consisting of roof bolts, steel mesh and support cables (Fig 7).

Analysis and results

For comparative purposes, signal power loss was determined from the main entry into the crosscut at the point where propagation once again exhibited far-zone behavior. However, the point in the crosscut at which propagation once again exhibited far-zone behavior is subjective. Also, with the Tx antenna located near the corner, propagation behavior was often such that there was no apparent around-the-corner signal loss.

The top graph in Fig 8 shows a typically plotted measurement result of around-the-corner propagation with the Tx antenna located far from the corner, 90 m (195 ft) away. In this figure, the point at which the Tx and Rx antennas became non-line-of-sight can be easily determined. In contrast, determining the point at which the effect of turning the corner had diminished the propagation behavior once again exhibited far-zone behavior is subjective. In the case shown in the top graph of Fig 8, it was concluded that the far-zone propagation behavior resumed at about 100 m (328 ft) and that the estimated power loss around-the-corner was approximately 50 dB, noted as "corner loss" in the figure.

The bottom graph in Fig. 8 is an example of propagation behavior with no apparent around-the-corner loss. With the Tx antenna located 20 m (66 ft) from the corner, there was no definitive point at which the Tx and Rx antennas became non-line-of-sight, and the near-zone propagation behavior continued well into the crosscut. Due to this propagation behavior, around-the-corner signal loss with the Tx antenna located near the corner was only determined for the measurements taken at Grand Coulee Dam. The fact that Grand Coulee Dam had discernable around-the-corner losses with the Tx antenna located near the corner could be attributed to the smooth walls, well-defined corners and smaller dimensions of the

concrete tunnels. Selected propagation measurement data with antenna polarization oriented for the best performance in the main entry or tunnel are shown in Figs. 9, 10 and 11 (Emslie, Lagace and Strong, 1975; Zhou et al., 2013). Data for the 90-m and 70-m Tx locations are shown on the left, marked as (a), and those for the 20-m (66-ft) and 10-m (33-ft) locations are shown on the right, marked as (b). Vertical dashed lines indicate the center of the crosscut relative to the Tx antenna.

The 90-m (295-ft) and 70-m (230-ft) Tx location measurement data show not only the ease in determining the point at which the Tx and Rx antennas became non-line-of-sight but also the ease in determining the near- and far-zone regions of line-of-sight propagation in the main entry or tunnel (Dudley, 2007; Hrovat and Javornik, 2014). In contrast, the 20-m (66-ft) and 10-m (33-ft) measurement data demonstrate that as the main entry or tunnel dimensions increase, around-the-corner loss becomes much less evident and the near- and far-zone regions of line-of-sight propagation are not as easily identified.

Summary of around-the-corner RF propagation

Tables 1 and 2 summarize around-the-corner RF propagation signal loss for the far and near Tx locations, respectively. Tables 3 and 4 give the distances into the crosscut or side tunnel from the centerline of the main entry or tunnel used to determine the around-the-corner signal losses summarized in Tables 1 and 2. (Due to the previously discussed propagation behaviors with the Tx antenna located near the corner, only data for the Grand Coulee Dam are presented in Tables 2 and 4.)

Specific antenna polarizations follow the naming configuration indicated by “TxRxRx,” where Tx is the Tx antenna polarization in the main tunnel or entry, the first Rx is the antenna polarization in the main tunnel or entry, and the second Rx is the antenna polarization in the side tunnel or crosscut. The antenna polarizations follow three designations based on orientation: (V) for vertical, (H) for horizontal and (L) for longitudinal. For example, “HHL” would indicate the Tx antenna was horizontally polarized in the main entry and the Rx antenna was horizontally polarized in the main entry, then oriented longitudinally upon entering the crosscut.

Around-the-corner loss data with antenna polarization oriented for the best RF propagation performance in the main tunnel or entry are shown with shaded backgrounds (Emslie, Lagace and Strong, 1975; Zhou et al., 2013). However, it is important to note that antenna polarization oriented for best propagation performance in the main tunnel or entry may not equate to best propagation performance around the corner.

Discussion

The work by Emslie, Lagace and Strong (1975) is one of the few prior studies that addresses around-the-corner propagation. While focusing primarily on the theoretical modeling of radio signal propagation in tunnels, it did present measurement results of around-the-corner propagation at two frequencies for horizontal polarization. However, the results are coarse, limited by the measurement methods available at the time. By comparison, the measurement results presented in this paper are more extensive — including four frequencies spanning a

wide bandwidth of more than 5 GHz at three polarization combinations — and more accurate due to the use of the new measurement method introduced. Although the results in this paper cannot be directly compared with those of Emslie, Lagace and Strong (1975) as the measurements were taken in different mines, both show there is a significant signal level loss from the main entry into the crosscut as line-of-sight propagation is lost.

As described in Zhou et al. (2016), around-the-corner signal propagation can be divided into three primary parts: propagation in the main entry, transition from propagation in the main entry to propagation into the crosscut, and propagation in the crosscut itself. Propagation in both the main entry and crosscut is determined by three principal factors: frequency, antenna polarization, and cross-sectional dimensions of the main entry or crosscut (Emslie, Lagace and Strong, 1975; Zhou et al., 2013). The transitional propagation signal loss from the main entry into the crosscut is composed of two parts. The first part, having the more significant signal loss, is due to the modal coupling between the main entry and crosscut and can be predicted by the uniform theory of diffraction (Zhou et al., 2016). The second part, having a less significant signal loss, can be attributed to an additional near-zone region of propagation as the signal begins propagation in the crosscut (Emslie, Lagace and Strong, 1975; Zhou et al., 2016). As noted in the analysis and results section, with the Tx antenna located near the corner, there appears to be no identifiable around-the-corner signal loss that can be attributed to modal coupling, only a smooth transition from the first to second near zones of propagation.

Conclusion

Radio signal propagation in an underground mining environment is generally different from that on the surface and has not been well understood. In this paper, a simple test apparatus is introduced to measure UHF/SHF signal propagation from an entry into a crosscut in mines and tunnels. Beginning with a simple concrete tunnel and progressing to the complex environment of an operating coal mine, the test apparatus was used to make comprehensive around-the-corner signal propagation measurements in a variety of underground environments. The mines and tunnels reported include a concrete dam, a small research coal mine and a typical high-seam western coal mine.

The measurement results reveal that many factors contribute to around-the-corner signal losses including tunnel dimensions, frequency, and antenna polarization. The presented data serve to improve the general understanding on how UHF/SHF signals couple from a main entry to cross cuts in underground mining environments, and can be used to validate theoretical around-the-corner coupling models. This should ultimately result in more reliable wireless links and enhanced performance of communications and tracking systems.

References

Dudley DG, Lienard M, Mahmoud SF, Degauque P. Wireless propagation in tunnels. IEEE Antennas and Propagation Magazine. 2007 Apr.49:11–26.

Hrovat A, Javornik T. A Survey of radio propagation modeling for tunnels. IEEE Communications Surveys & Tutorials. 2014; 16(2)

Emslie A, Lagace R, Strong P. Theory of the propagation of UHF radio waves in coal mine tunnels. IEEE Transactions on Antennas and Propagation. 1975; 23:192–205.

Zhou C, Waynert J, Plass T, Jacksha R. Attenuation constants of radio waves in lossy-walled rectangular waveguides. Progress In Electromagnetics Research (PIER). 2013; 142:75–105.

Zhou, C., Jacksha, R., Reyes, M. IEEE Radio and Wireless Symposium. Austin TX: 2016 Jan. Measurement and modeling of radio propagation from a primary tunnel to cross junctions. 2016

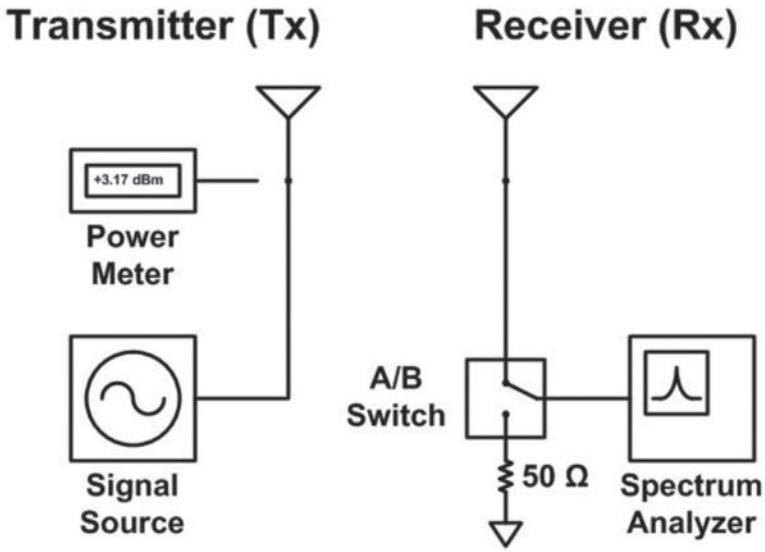

Figure 1.
Measurement system block diagram.

Figure 2.
RF measurement system hardware.

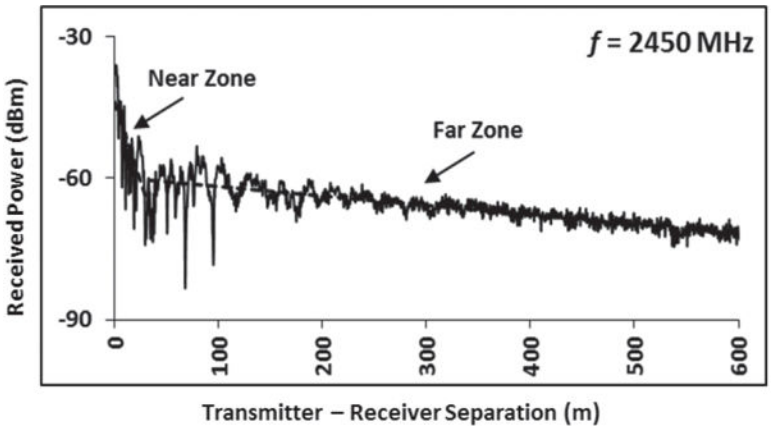

Figure 3.
Near- and far-zone regions of line-of-sight RF propagation in a concrete tunnel.

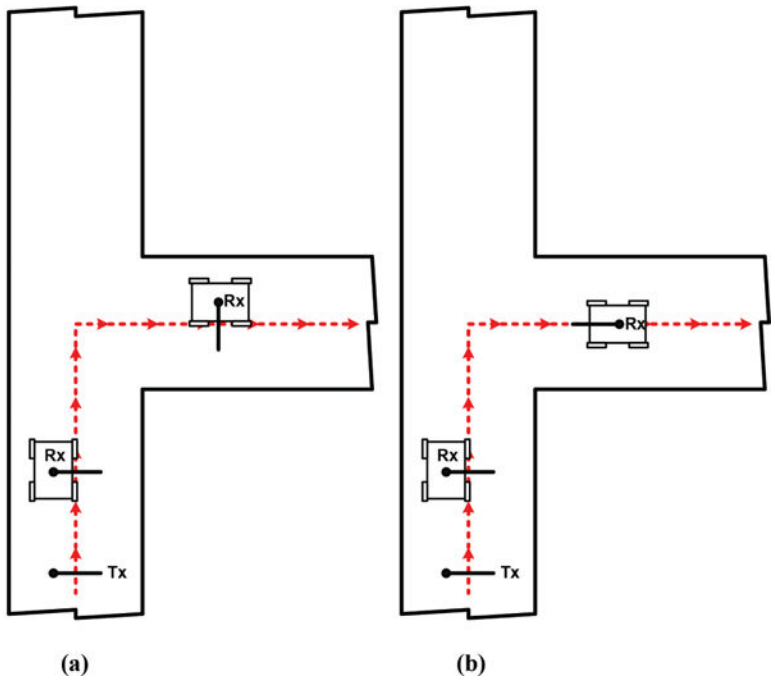

Figure 4.

Antenna alignment: (a) Tx horizontal, Rx horizontal, Rx horizontal and (b) Tx horizontal, Rx horizontal, Rx longitudinal.

Figure 5.
Grand Coulee Dam main tunnel.

Figure 6.
Safety Research Coal Mine main entry.

Figure 7.
Western high-seam coal mine main entry.

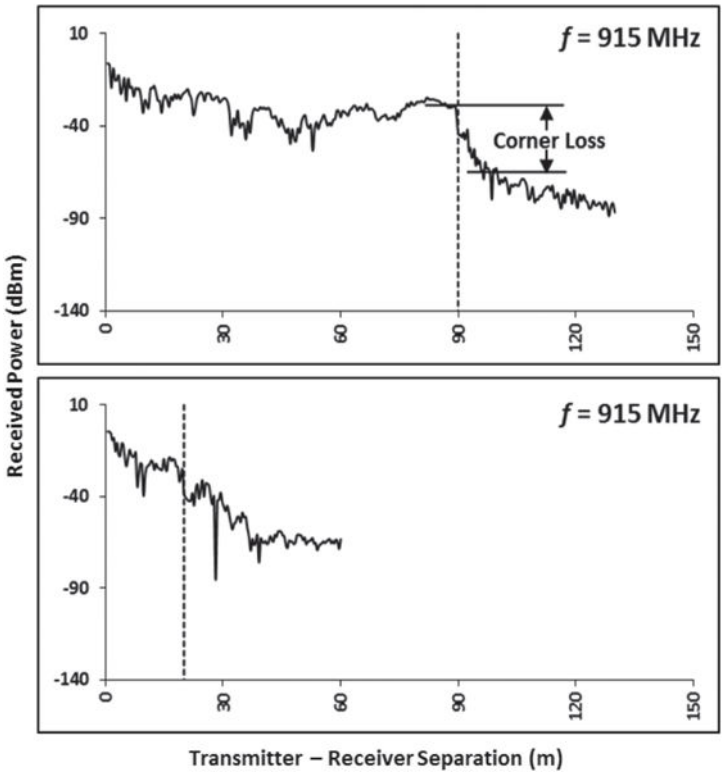

Figure 8.
Typical results for two Tx antenna locations relative to the corner: (a) 90 m and (b) 20 m from corner.

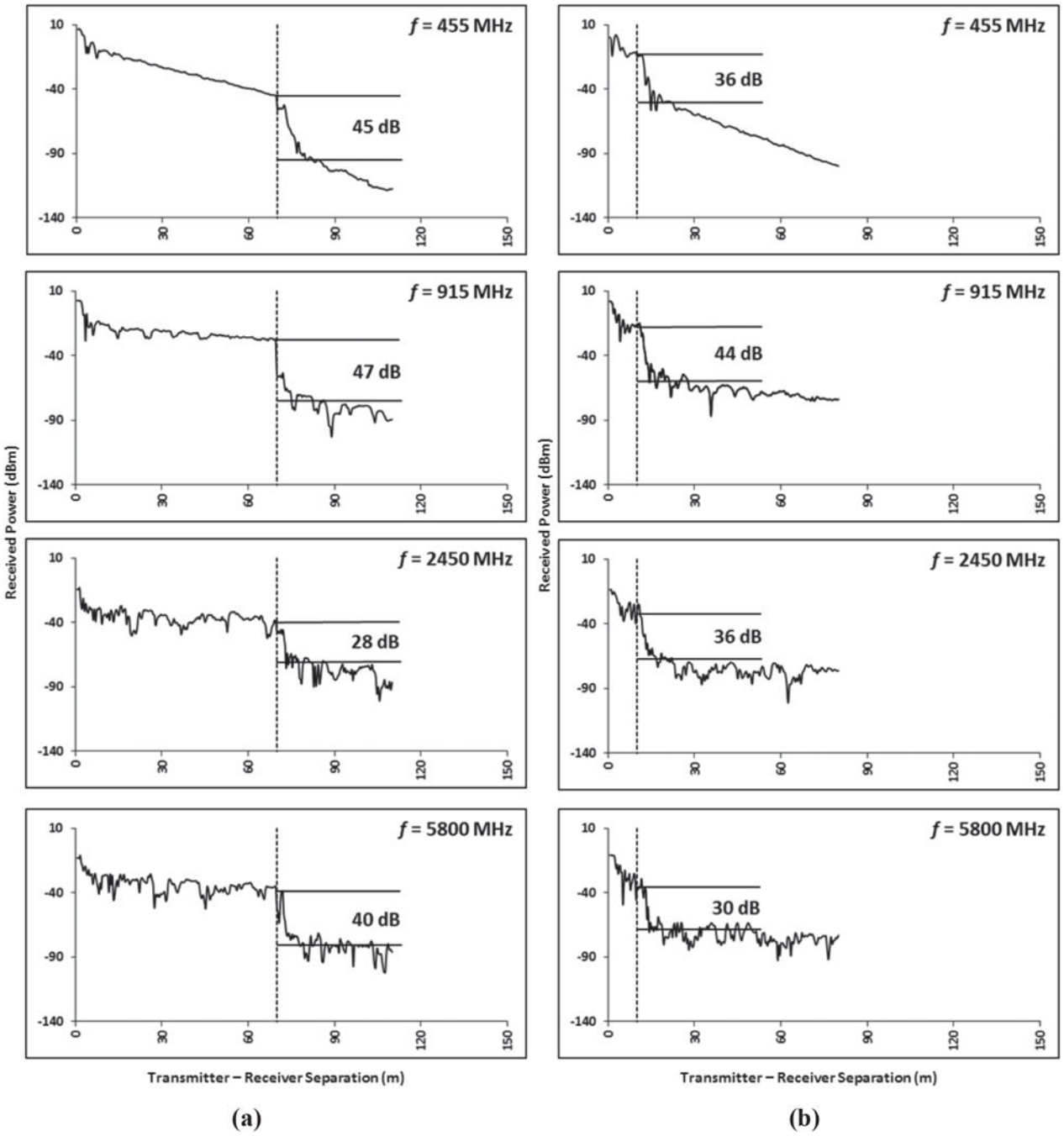

Figure 9.
Grand Coulee Dam vertical polarization Tx: (a) 70 m from corner and (b) 10 m from corner.

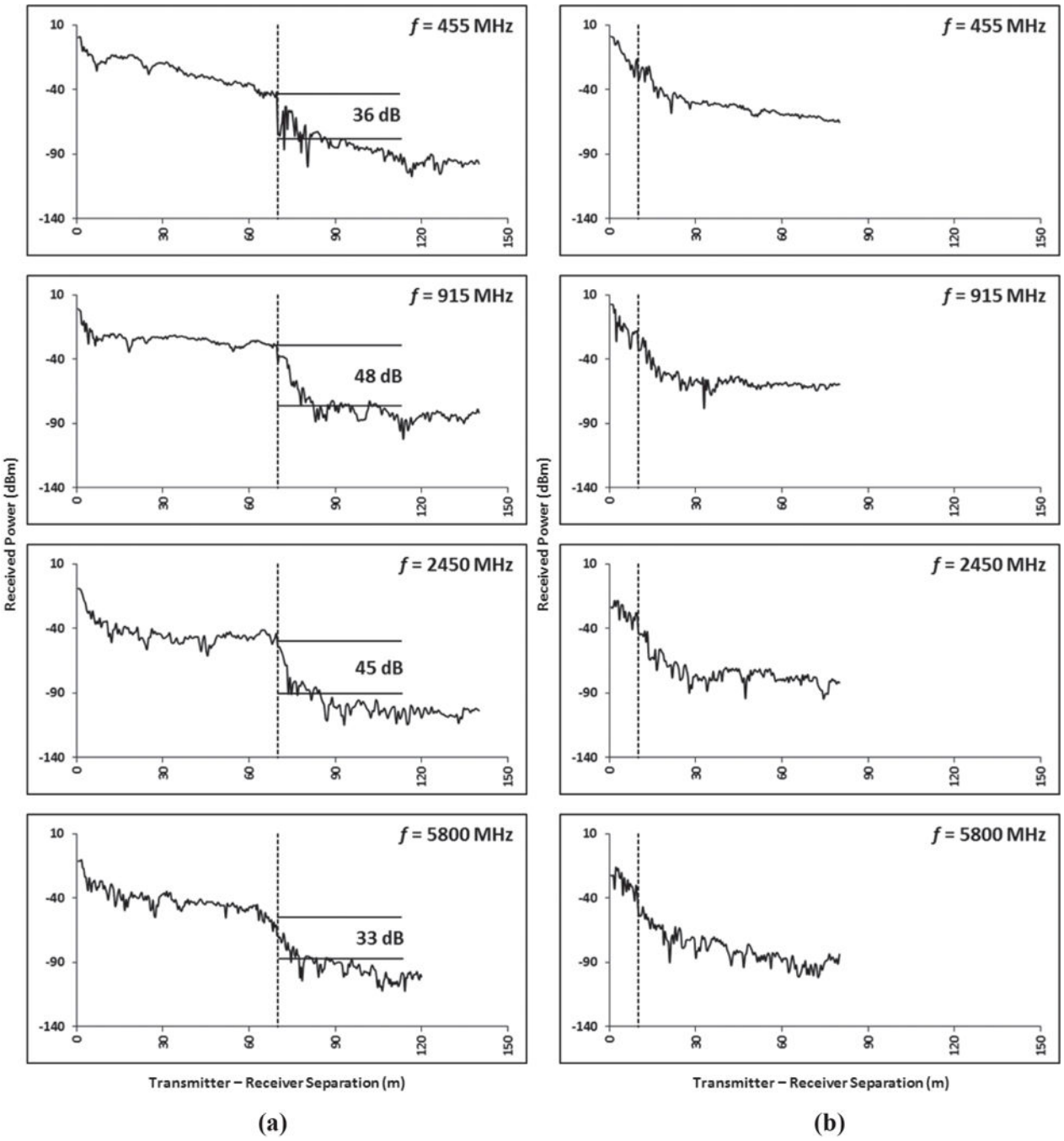

Figure 10.
Safety Research Coal Mine horizontal polarization Tx: (a) 70 m from corner and (b) 10 m from corner.

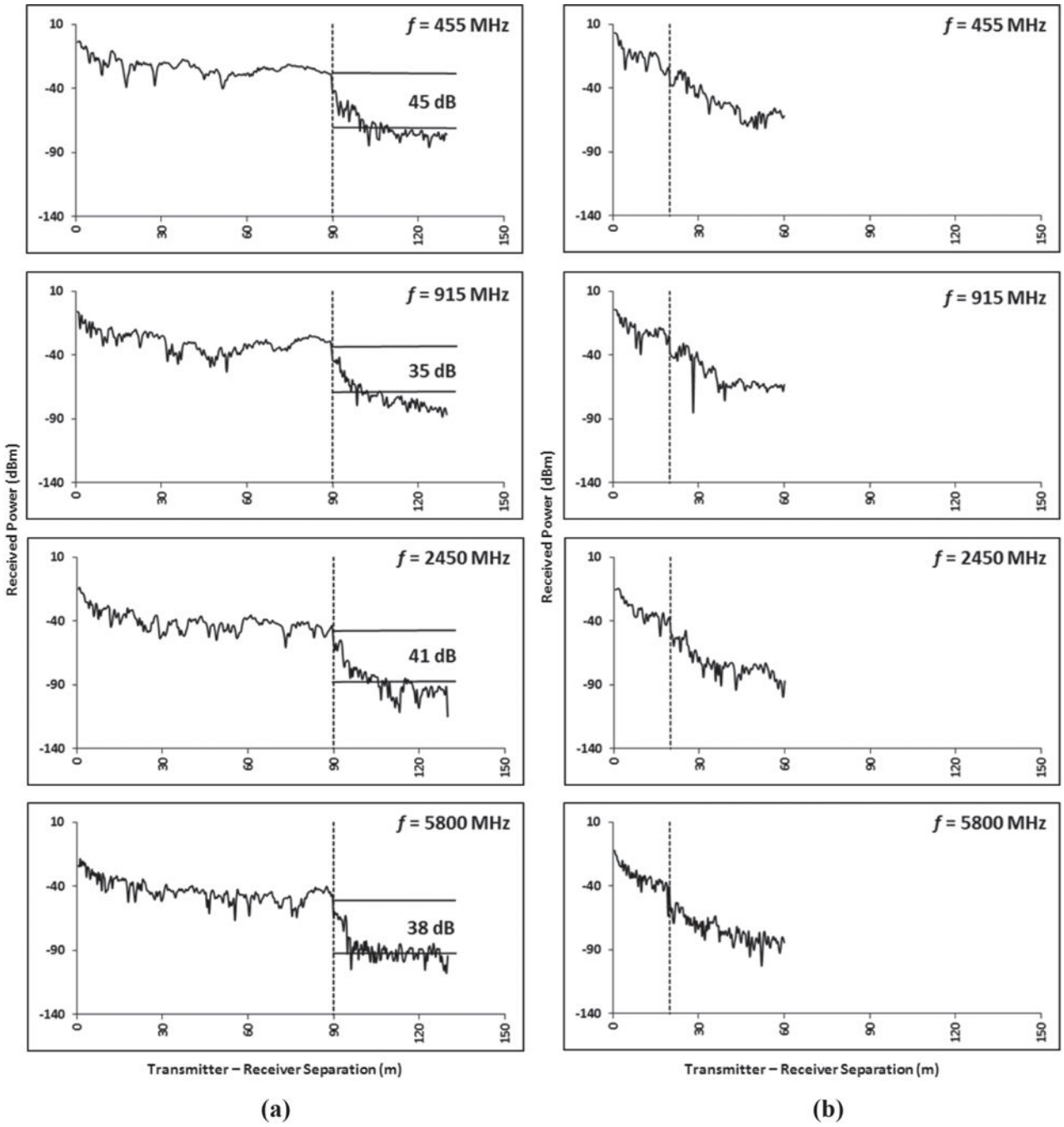

Figure 11.
High-seam western coal mine collinear horizontal polarization: (a) 90 m from corner and (b) 20 m from corner.

Table 1

Around-the-corner RF propagation signal loss (dB) at 70 m and 90 m from corner.

Site	W × H (m) (Main) (Side)	455 MHz Antenna polarization (TxRxRx)			915 MHz Antenna polarization (TxRxRx)			2450 MHz Antenna polarization (TxRxRx)			5800 MHz Antenna polarization (TxRxRx)		
		VVV	HHH	HHL	VVV	HHH	HHL	VVV	HHH	HHL	VVV	HHH	HHL
Coulee Dam	1.8 × 2.4 1.5 × 2.1	45	38	38	47	43	55	28	53	58	40	56	75
SRCM	2.7 × 1.6–2.0 2.7 × 1.6–2.0	10	36	48	40	48	55	47	45	40	33	33	50
Coal mine	5.6–5.9 × 2.7–3.4 5.2–5.3 × 2.4–2.7	30	45	53	30	35	48	27	41	50	32	38	52

Table 2

Around-the-corner RF propagation signal loss (dB) at 10 m from corner.

Site	W × H (m) (Main) (Side)	455 MHz Antenna polarization (TxRxRx)			915 MHz Antenna polarization (TxRxRx)			2450 MHz Antenna polarization (TxRxRx)			5800 MHz Antenna polarization (TxRxRx)		
		VVV	HHH	HHL	VVV	HHH	HHL	VVV	HHH	HHL	VVV	HHH	HHL
Coulee Dam	1.8 × 2.4 1.5 × 2.1	36	43	39	44	40	50	36	No data	53	30	39	53

Table 3

Distance into crosscut or side tunnel used for loss calculations at 70m and 90 m from corner.

Site	W × H (m) (Main) (Side)	455 MHz Antenna polarization (TxRxRx)			915 MHz Antenna polarization (TxRxRx)			2450 MHz Antenna polarization (TxRxRx)			5800 MHz Antenna polarization (TxRxRx)		
		VVV	HHH	HHL	VVV	HHH	HHL	VVV	HHH	HHL	VVV	HHH	HHL
Coulee Dam	1.8 × 2.4 1.5 × 2.1	11	11	5	6	5	9	3	5	5	9	6	10
SRCM	2.7 × 1.6–2.0 2.7 × 1.6–2.0	6	8	10	9	8	9	10	7	7	10	9	9
Coal mine	5.6–5.9 × 2.7–3.4 5.2–5.3 × 2.4–2.7	7	10	12	10	10	13	7	10	14	8	7	14

Table 4

Distance into crosscut or side tunnel used for loss calculations at 10 m from corner.

Site	W × H (m) (Main) (Side)	455 MHz Antenna polarization (TxRxRx)			915 MHz Antenna polarization (TxRxRx)			2450 MHz Antenna polarization (TxRxRx)			5800 MHz Antenna polarization (TxRxRx)		
		VVV	HHH	HHL	VVV	HHH	HHL	VVV	HHH	HHL	VVV	HHH	HHL
Coulee Dam	1.8 × 2.4 1.5 × 2.1	10	10	10	11	11	8	10	No data	10	5	10	12